Achromatic diffraction from polarization gratings with high efficiency

Chulwoo Oh and Michael J. Escuti*

Department of Electrical and Computer Engineering, North Carolina State University,
Raleigh, North Carolina 27695, USA
*Corresponding author: mjescuti@ncsu.edu

We demonstrate a broadband, thin-film, polarizing beam splitter based on an anisotropic diffraction grating composed of reactive mesogens (polymerizable liquid crystals). This achromatic polarization grating (PG) manifests high diffraction efficiency ($\sim$100%) and high extinction ratio ($\geq$1000:1) in both theory and experiment. We show an operational bandwidth $\Delta\lambda/\lambda_0 \sim 56\%$ (roughly spanning visible wavelength range) that represents more than a fourfold increase of bandwidth over conventional PGs (and significantly larger than any other grating). The diffraction angle and operational region (visible, near-infrared, midwave infrared, and ultraviolet wavelengths) may be easily tailored during fabrication. The essence of the achromatic design is a stack of two chiral PGs with an opposite twist sense and employs the principle of retardation compensation. We fully characterize its optical properties and derive the theoretical diffraction behavior.
© 2008 Optical Society of America

OCIS codes: 050.1950, 230.1360, 260.5430, 090.1970.

The management and measurement of polarized light is essential in a wide range of applications including liquid crystal (LC) displays, polarimetry, astronomy, optical fiber communications, quantum computing, and microscopy. While splitting light into orthogonal polarizations may be accomplished using glass beam splitters (e.g., Wollaston or Glan), this is in many cases undesirable owing to their large physical size/weight or limited operational wavelength range. Polarization gratings (PGs) are efficient polarization-sensitive diffractive thin films [1–4] and novel electro-optical switches [5–8] that can diffract with $\sim$100% efficiency into the first orders with polarization selectivity analogous to glass beam splitters. One conventional profile is the "circular PG" [1,4] and consists of a spiraling, in-plane, linear birefringence that is uniform in the z dimension. However, its high diffraction efficiency occurs only over a modest bandwidth, a limitation [9] that applies to practically all gratings (Bragg or Raman–Nath).

In this Letter, we demonstrate an achromatic PG formed with reactive mesogens (RMs) (polymerizable LCs) [10,11] that accomplishes both chromatic and polarization separation simultaneously. This periodic anisotropic profile manifests $\sim$100% efficiency across the entire visible wavelength range (more than a fourfold increase in bandwidth over circular PGs), achieving achromatic diffraction by compensating the chromatic dispersion of retardation using the effect of twist.

This achromatic PG comprises two antisymmetric chiral circular PGs with an opposite twist sense, where the nematic director **n** follows

$$\mathbf{n}(x,z) = [\cos\phi(x,z), \quad \sin\phi(x,z), \quad 0], \tag{1a}$$

$$\phi(x,z) = \begin{cases} \pi x/\Lambda + \Phi z/d & \text{if } 0 \leq z \leq d \\ \pi x/\Lambda - \Phi z/d + 2\Phi & \text{if } d < z \leq 2d \end{cases}, \tag{1b}$$

where ϕ is the azimuth angle of the director field, Λ is the grating period, d is the thickness, and Φ is the

twist angle of each chiral layer. Figures 1(a) and 1(b) illustrate this profile. RMs [10,11] are ideal to create this anisotropy pattern, since their orientation can be initially established by surfaces and chiral dopants and indefinitely fixed via photopolymerization.

The diffraction efficiency η_m of order m may be calculated using the Jones calculus under the paraxial (small-angle) approximation, a method employed previously by several authors for conventional PGs [2,3,12]. Since the derivation for our anisotropy profile [Eq. (1)] involves lengthy expressions, here we will only summarize the approach and include the final result (refer to [13] for details). First, we find the spatially varying 2×2 transfer matrix $\mathbf{T}_{\text{APG}}(x)$, incorporating all grating geometry and material anisotropy. The achromatic PG profile is expressed as multiple thin layers of circular PGs with a small lateral phase shift between them, akin to the analysis of twisted nematic LC modes as stratified media [14]. Second, we find the electric field of diffraction
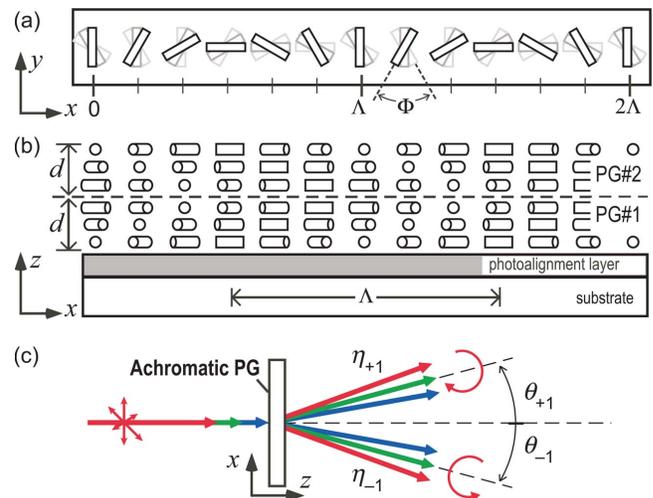

Fig. 1. (Color online) Achromatic PG. Nematic director profile (a) plan view and (b) side view. (c) Diffraction geometry (note only the $m = \pm1$ orders emerge).

© 2008 Optical Society of America

order m far from the grating as $\mathbf{D}_m$ $=(1/\Lambda)\int_0^\Lambda \mathbf{T}_{\mathrm{APG}}(x)\mathbf{E}_{in}e^{-i2\pi mx/\Lambda}dx$. Finally, we determine the diffraction efficiency as $\eta_m=|\mathbf{D}_m|^2/|\mathbf{E}_{in}|^2$, which may be analytically summarized by the following:

$$\eta_0 = [\cos^2 X + (\Phi^2 - \Gamma^2)\mathrm{sinc}^2 X]^2, \qquad (2a)$$

$$\eta_{\pm 1} = A^2\left(\frac{1 \mp S_3'}{2}\right)(\cos^2 X + \Phi^2 \mathrm{sinc}^2 X), \qquad (2b)$$

where $\Gamma = \pi\Delta nd/\lambda$, $X=\sqrt{\Phi^2+\Gamma^2}$, $A=2\Gamma\,\mathrm{sinc}\,X$, and $\mathrm{sinc}\,X \equiv (\sin X)/X$. The term $S_3'=S_3/S_0$ is a normalized Stokes parameter. The grating equation $\sin\theta_m = m\lambda/\Lambda \pm \sin\theta_{in}$ governs diffraction angles [Fig. 1(c)].

Several important properties should be noted in Eqs. (2a) and (2b) and in [13]. First, only three diffraction orders (0 and ±1) exist, which depend on both the retardation $\Delta nd/\lambda$ and the twist angle Φ. We will show that $\Sigma\,\eta_{\pm 1}\approx 100\%$ over a wide wavelength range by balancing the effect of retardation and twist. Second, the first orders have orthogonal circular polarizations [Fig. 1(c)]. Third, the first-order efficiencies are strongly sensitive to the incident polarization state through S_3' (akin to circular PGs). Overall, we understand the achromaticity of the two antisymmetric chiral layers as self-compensation, via counteracting chromatic dispersions in the linear and twist-induced circular birefringences [15].

To enable a quantitative evaluation, we define bandwidth as $\Delta\lambda/\lambda_0$, the ratio of the spectral range $\Delta\lambda$ (over which high diffraction efficiency $\Sigma\,\eta_{\pm 1} \geqslant 99\%$ occurs) to the center wavelength λ_0. We employ Eq. (2b) to generate a map of total first-order diffraction efficiency as a function of the retardation and the twist angle [shown in Fig. 2(a)]. The maximum bandwidth ($\approx 56.1\%$) is found when $\Phi=70°$. Note this is more than a fourfold enhancement as

compared with a conventional circular PG ($\approx 12.8\%$), as shown in Fig. 2(b) with relative bandwidths highlighted.

We have experimentally realized this achromatic PG formed as an RM film by polarization holography and photoalignment techniques. In a recent work [3], we fabricated defect-free circular PGs in RM thin-films with ultrahigh efficiency (more than 99%) and low scattering by materials and processing optimization.

Here, we apply the same [3] holographic and multilayer principles to fabricate achromatic PGs. In particular, we utilized a linear photopolymerizable polymer (LPP) [16] ROP-103 (Rolic) as a photoalignment material. The surface alignment pattern with a period of $\Lambda=6.5\ \mu$m was recorded in the LPP layer by orthogonal circular-polarized beams from an He–Cd laser (at 325 nm). After holographic exposure, RM films were spin-coated onto the LPP-coated substrate. The first PG layer was composed of the RM prepolymer–solvent mixture RMS03-001 (Merck, $\Delta n \approx 0.159$ at 589 nm) doped with a small amount (0.25%) of the chiral molecule CB15 (Merck, right-handed). A thickness $d \approx 1.7\ \mu$m was chosen so that half-wave retardation $\Gamma = \pi/2$ (at $\lambda \approx 550$ nm) and a twist $\Phi = +70°$ occurred simultaneously. The second PG layer was deposited directly onto the top of the first and was composed of RMS03-001 doped with a small amount (0.34%) of the chiral molecule ZLI-811 (Merck, left-handed), resulting in the same thickness and opposite twist angle ($\Phi=-70°$). As these RM films are highly cross-linked acrylate films, they are known [11,16] to have high thermal and optical stabilities. Reproducibility and fabrication process sensitivity are similar to other spin-coated RM films.

These achromatic PGs exhibit practically ideal properties with high first-order efficiency, high polarization-selectivity, low scattering, and low non-first-order leakage. As shown in Fig. 3, nearly 100% of incident light can be directed into the first orders alone for both light-emitting diode (LED) and laser
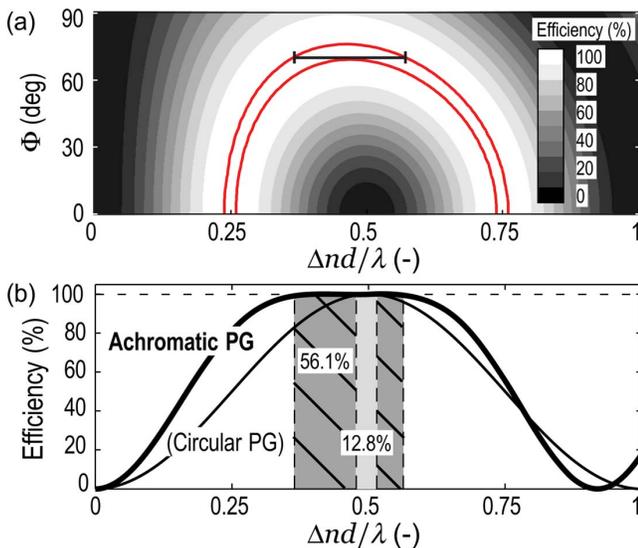

Fig. 2. (Color online) Theoretical diffraction of the achromatic PG. (a) First-order efficiency spectra versus twist angle Φ ($\Sigma\,\eta_{\pm 1} \geqslant 99\%$, outlined region). (b) First-order efficiency spectrum for $\Phi=70°$ compared with the circular PG.
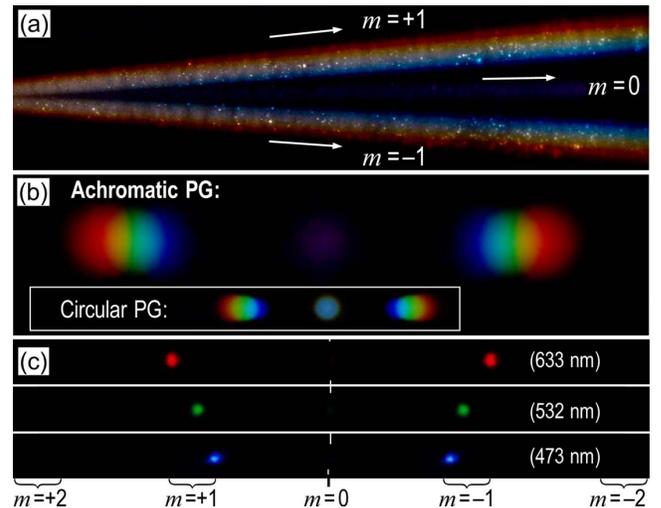

Fig. 3. (Color online) Photographs of achromatic PG diffraction. Unpolarized white LED light as seen from (a) plan view (intersecting a white card) and (b) projected screen view. (c) Linearly polarized laser light ($\Lambda=6.5\ \mu$m).

light [wavelengths in Fig. 3(c)]. Note the substantially reduced zero-order leakage of the achromatic PG compared with the circular PG [see Fig. 3(b)]. Note also that both unpolarized and linearly polarized light are split equally (since $S'_3 = 0$).

The measured diffraction efficiencies of the achromatic PG with circularly polarized incident laser light are summarized in Fig. 4(a). Very high efficiencies of $\geq 99\%$ within a single order ($m = +1$) were observed throughout the visible spectrum (since $S'_3 = -1$). Most other diffraction orders ($m = -2, -1, +2$, and higher) manifest $\leq 0.1\%$, while the worst case leakage of $< 0.7\%$ arose in the zero order ($m = 0$) for the green wavelength. We define diffraction efficiency as $\eta_m = I_m / I_{\mathrm{REF}}$, where I_m is the measured intensity of the mth transmitted diffracted order and where I_{REF} is a reference transmission intensity for a glass substrate. Incoherent scattering was measured as $\leq 0.3\%$ above 400 nm.

We also measured the polarization sensitivity of the first orders by arranging and rotating quarter-wave plates in between the achromatic PG and the linearly polarized lasers. Figure 4(b) shows the +1-order response for the red laser (as the best example wavelength). The efficiency varies as the incident light is varied from linear ($\approx 50\%$), to circular ($\approx 99.5\%$, right-handed), to linear ($\approx 50\%$), and finally back to circular ($\approx 0.05\%$, left-handed). The extinction ratio is therefore $99.5/0.05 \simeq 2000 : 1$ (or 33 dB), an excellent measure for polarizing beam splitters of any kind. The green and blue wavelengths were slightly lower but nevertheless maintained $\geq 1000 : 1$ (30 dB) extinction ratios.

Finally, we examined the spectrum of the achromatic PG by measuring η_0 using a spectrophotometer (with $\eta_{|m| \geq 1}$ blocked) and estimating $\Sigma \eta_{\pm 1} \simeq 100\% - \eta_0$ (due to the difficulty of its direct measurement). The result is shown in Fig. 4(c) with the exact efficiencies measured using lasers (which match up well). The achromatic PG clearly manifests high diffraction efficiency ($\geq 99\%$) across almost all visible wavelengths, which is a substantial improvement over the conventional circular PG.

In sum, we have demonstrated an achromatic PG as reactive mesogens that manifests high diffraction efficiency ($\sim 100\%$) and high extinction ratio ($\geq 1000 : 1$) in both theory and experiment. We show an operational bandwidth $\Delta \lambda / \lambda_0 \sim 56\%$ (roughly spanning visible wavelength range). As a polymer thin-film analog to the Wollaston prism, this broadband polarizing beam splitter should find diverse utility throughout optics and photonics.
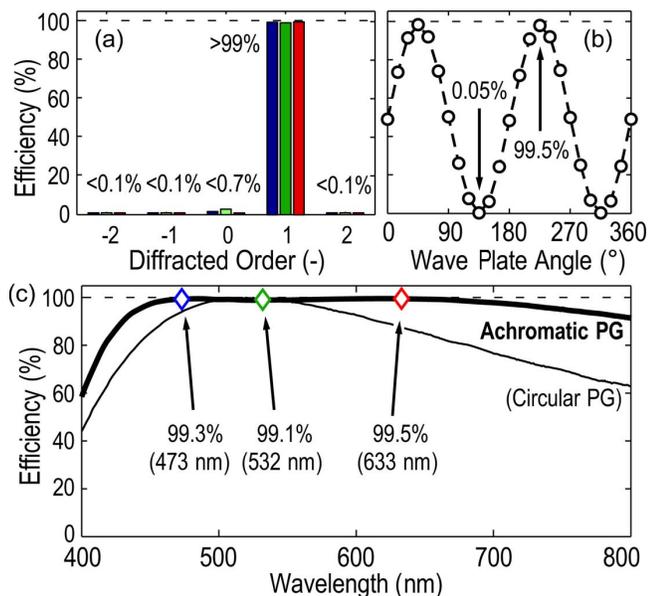
Fig. 4. (Color online) Measured diffraction of the achromatic PG. (a) Efficiencies with circularly polarized incident laser light [same wavelengths as in Fig. 3(c)]. (b) Polarization sensitivity of the $m = +1$ order with a rotating quarter-wave plate. (c) First-order efficiency spectrum from spectrometer (curves) and laser (diamonds) measurements.

References

1. L. Nikolova and T. Todorov, Opt. Acta **31**, 579 (1984).
2. J. Tervo and J. Turunen, Opt. Lett. **25**, 785 (2000).
3. M. J. Escuti, C. Oh, C. Sanchez, C. W. M. Bastiaansen, and D. J. Broer, Proc. SPIE **6302**, 632614 (2006).
4. C. Oh and M. J. Escuti, Phys. Rev. A **76**, 043815 (2007).
5. J. N. Eakin, Y. Xie, R. A. Pelcovits, M. D. Radcliffe, and G. P. Crawford, Appl. Phys. Lett. **85**, 1671 (2004).
6. H. Sarkissian, S. V. Serak, N. V. Tabiryan, L. B. Glebov, V. Rotar, and B. Y. Zeldovich, Opt. Lett. **31**, 2248 (2006).
7. R. K. Komanduri, W. M. Jones, C. Oh, and M. J. Escuti, J. Soc. Inf. Disp. **15**, 589 (2007).
8. C. Provenzano, P. Pagliusi, and G. Cipparrone, Appl. Phys. Lett. **89**, 121105 (2006).
9. H. Lajunen, J. Tervo, and J. Turunen, Opt. Lett. **29**, 803 (2004).
10. D. J. Broer, Macromol. Chem. Phys. **190**, 2255 (1989).
11. S. M. Kelly, J. Mater. Chem. **5**, 2047 (1995).
12. C. van Heesch, Ph.D. dissertation (Eindhoven University of Technology, 2007).
13. C. Oh and M. J. Escuti, Proc. SPIE **6682**, 668211 (2007).
14. P. Yeh and C. Gu, *Optics of Liquid Crystal Displays* (Wiley, 1999).
15. T. Scheffer and J. Nehring, Annu. Rev. Mater. Sci. **27**, 555 (1997).
16. M. Schadt, H. Seiberle, and A. Schuster, Nature **381**, 123102 (1996).